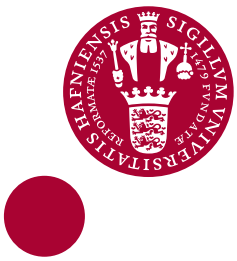

Gene structure and expression pattern analysis of three monodehydroascorbate reductase (Mdhar) genes in Physcomitrella patens
implications for the evolution of the MDHAR family in plants

Lunde, Christina; Baumann, Ute; Shirley, Neil J.; Drew, Damian P.; Fincher, Geoffrey B.

Published in:
Plant Molecular Biology

DOI:
10.1007/s11103-005-3881-8

Publication date:
2006

Document version
Early version, also known as pre-print

Gene structure and expression pattern analysis of three monodehydroascorbate reductase (*Mdhar*) genes in *Physcomitrella patens*: Implications for the evolution of the MDHAR family in plants

Christina Lunde[2]*, Ute Baumann[1], Neil J. Shirley[1], Damian P. Drew[1] and Geoffrey B. Fincher[1]

[1]Australian Centre for Plant Functional Genomics

School of Agriculture and Wine

University of Adelaide

Waite Campus

Glen Osmond SA 5064

Australia

[2]*Address for Correspondence; Present address

Plant Biochemistry Laboratory, Department of Plant Biology

The Royal Veterinary and Agricultural University

40 Thorvaldsensvej

DK-1871 Frederiksberg C, Copenhagen, Denmark

Tel: +45 35 28 33 17

Fax: +45 35 28 33 33

E-mail: chlu@kvl.dk

Accession numbers; DQ159869, DQ159870, DQ159871

Abstract

The ascorbate-glutathione pathway plays a major role in the detoxification of reactive oxygen species (ROS) in vascular plants. One of the key enzymes in this pathway is monodehydroascorbate reductase (MDHAR), a FAD enzyme that catalyses the reduction of the monodehydroascorbate radical. To elucidate the evolution and functional role of MDHAR we identified and characterised MDHARs from the moss *Physcomitrella patens*. Expressed sequence tag (EST) databases containing approximately 100.000 ESTs from *Physcomitrella* were searched and three isoforms of monodehydroascorbate reductase (PpMDHAR1, PpMDHAR2 and PpMDHAR3) were identified. In vascular plants MDHAR is found in the cytosol, chloroplast, mitochondria and peroxisome. Surprisingly, all three PpMDHARs resembled the cytosolic isoforms from vascular plants lacking the NH_2-terminal or COOH-terminal extension found in organelle targeted MDHARs. The number and position of introns was also conserved between PpMDHARs and cytosolic MDHARs from vascular plants. Phylogenetic analysis revealed that cytosolic MDHARs are monophyletic in origin and the ancestral gene evolved before the divergence of bryophytes more than 400 million years ago. Transcript analyses showed that expression of *PpMdhar1* and *PpMdhar3* was increased up to 5-fold under salt stress, osmotic stress or upon exposure to abscisic acid. In contrast, *PpMdhar* transcription levels were unchanged upon chilling, UV-B exposure or oxidative stress. The conservation of cytosolic MDHAR in the land-plant lineage and the transcriptional upregulation under water deficiency suggest that the evolution of cytosolic MDHAR played an essential role in stress protection for land plants when they inhabited the dry terrestrial environment.

Keywords: abiotic stress; abscisic acid; alternative splicing; ascorbate; phylogenetic; reactive oxygen species

Abbreviations: ABA, abscisic acid; APX, ascorbate peroxidase; DHAR, dehydroascorbate reductase; EST, expressed sequence tag; MeV, methyl viologen; MDHAR, monodehydroascorbate reductase; ROS, reactive oxygen species; SOD, superoxide dismutase

Introduction

Bryophytes originated 400-450 million years ago and represent one of the oldest groups of land plants (Kenrick and Crane, 1997). They are now found in a wide range of habitats throughout the world from Antarctica to the tropics. As one of the first land plants, they faced numerous and extreme environmental challenges, including exposure to high intensities of UV, large variations in temperature and lack of water. Their successful adaptation can be attributed to the acquisition of resistance to these abiotic stresses. In comparison to vascular plants, information as to how bryophytes cope with abiotic stresses is limited. A common secondary effect of a range of abiotic stresses is the generation of highly toxic reactive oxygen species (ROS). In vascular plants, the enzymes of the ascorbate-glutathione pathway play a significant role in the scavenging and detoxification of ROS (Mittler et al., 2004). Superoxide dismutase (SOD) and ascorbate peroxidase (APX) catalyse the conversion of O_2^- into the ascorbate free radical, monodehydroascorbate. Although ascorbate is found in high concentrations in plant cells, it has been estimated that under environmental stress such as high light exposure, the pool of ascorbate in the chloroplast is oxidised to monodehydroascorbate within a few minutes (Polle, 2001). It is therefore necessary for the survival of plants that monodehydroascorbate is reduced, thereby regenerating ascorbate.

In the chloroplast monodehydroascorbate is reduced to ascorbate by photoreduced ferredoxin at a high rate and this is likely to constitute the main pathway in the vicinity of the thylakoid membrane (Miyake and Asada, 1994). Away from the thylakoid membrane, reduction of monodehydroascorbate can occur via two enzymes in the ascorbate-glutathione pathway; dehydroascorbate reductase (DHAR) and monodehydroascorbate reductase (MDHAR) (Asada, 1999). Monodehydroascorbate can be reduced directly by MDHAR using NAD(P)H as an electron donor. Alternatively, two molecules of monodehydroascorbate can react non-enzymatically and spontaneously generate ascorbate and dehydroascorbate. In an enzyme-catalysed reaction, dehydroascorbate is reduced to ascorbate by DHAR, using glutathione as reductant. The relative

importance of the two pathways is not known, but the specific activity of MDHAR is 10 times higher than DHAR in both mitochondria and chloroplasts of tomato (Mittova et al., 2000). Computer simulations based on known enzyme concentrations and properties in the chloroplast lead to the conclusion that the majority of monodehydroascorbate is reduced by MDHAR (Polle, 2001).

The MDHAR enzyme activity is found across the plant and animal kingdoms (Arrigoni et al., 1981). However, plant MDHAR exhibits the highest level of sequence similarity with prokaryotic flavoenzymes such as iron-sulphur protein reductases. In angiosperms MDHAR activity has been detected in the chloroplast, mitochondria, peroxisome, cytosol, and associated with the plasma membrane and cell wall (Dalton et al, 1993; Leonardis et al., 1995; Bérczi and Møller, 1998; Mittova et al., 2000). The cytosolic MDHARs are composed of 433-436 amino acid residues while the mitochondrial and membrane-bound peroxisomal isoforms are 40-60 amino acid residues larger, due to a NH_2-terminal or COOH-terminal extension, respectively (Lisenbee et al., 2005; Sano et al., 2005). The targeting of MDHAR to either chloroplast or mitochondria is determined by the structural features of the NH_2-terminal transit peptide. In *Arabidopsis* and rice alternative transcription starts or alternative mRNA splicing determines the amino acid composition of the NH_2-terminus (Obara et al., 2002; Obara and Fukuda, 2004).

MDHAR has been purified from cucumber, soybean, spinach, potato and pea (Hossain et al., 1984; Hossain and Asada, 1985; Dalton et al., 1992; Murthy and Zilinskas, 1994, Sano et al., 1995). However, the MDHAR gene family has not yet been studied in a non-vascular plant and previous phylogenetic analysis only included sequences from angiosperms (Leterrier et al., 2005; Sano et al., 2005). As a representative of the bryophytes, the non-vascular *Physcomitrella patens* is a perfect candidate to study early adaptation to abiotic stress. In contrast to vascular plants, the life cycle of *Physcomitrella* comprises a predominantly haploid gametophytic phase and a short diploid sporophytic phase. The moss contains only a few cell types and most of its tissues consist of a single cell layer. Thus, it is relatively easy to generate homogeneous material and perform

controlled stress experiments, where all cells can be subjected to the imposed stress. In addition, *Physcomitrella* was recently shown to be highly tolerant to salt, drought and osmotic stresses (Frank et al., 2005). In the present study, we have identified three MDHAR isoforms in *Physcomitrella*. This allowed us to perform a phylogenetic analysis showing that two major duplication and diversification events gave rise to the chloroplast/mitochondrial, peroxisomal and cytosolic subfamilies. The expression pattern of the three *PpMdhar* genes was analysed and showed differential expression under abiotic stress. This functional specialisation does not appear to have been conserved, but has evolved several times during the evolution of land plants.

Materials and methods.

Plant material and growth conditions

Physcomitrella patens (Hedw.) derived from a wild type specimen collected in Gransden Wood in Huntingdonshire, UK (Ashton and Cove, 1977) was grown at 22 °C on cellophane disks placed on solid minimal media (Ashton et al., 1979), supplemented with ammonium tartrate (0.5 g/L). Standard growth conditions were 16 h white light (fluorescent tubes, GRO-LUX, 100 μmol m^{-2} sec^{-1}) and 8 h darkness. Stress experiments were carried out on protonema homogenised 7 days prior to the stress exposure, or on 5 week-old gametophytes. Abiotic stress was induced by transferring the cellophane with *Physcomitrella* protonema to media or filter disks containing 100 μM methyl viologen (Sigma), 60 or 100 mM NaCl, or 30 mM PEG 1,500 (Sigma). Extra $CaCl_2$ was added to the media containing NaCl to keep the level of available Ca^{++} constant. The amount of added $CaCl_2$ required was calculated using MinTeq ver2.30 (http://www.lwr.kth.se/English/OurSoftware/vminteq/). The osmolarity of PEG 1,500 and NaCl was calculated according to the Merck Index (11th ed. 1989, Merck and Co, Inc.). Cold stress was imposed by placing the plates on ice. UV-B stress was imposed by placing *Physcomitrella* under a UVLMS-38 lamp fitted with an 8 W 302 nm tube (Ultra-Violet Products, Cambridge, UK). The tissue was exposed to 0.23 mW cm^{-2} measured using an Optical Radiometer (MS-100, Ultra-Violet Products, Cambridge, UK) fitted with a UV-B sensor (MP-131). Hormone treatment was done by exposing tissue to 50 μM abscisic acid (Sigma). Samples were frozen in liquid nitrogen upon harvesting and stored at -80 C until RNA was extracted.

Cloning and sequencing of PpMdhar1, PpMdhar2 and PpMdhar3 from cDNAs and genomic DNA.

Expressed sequence tags (ESTs) encoding monodehydroascorbate reductases were obtained by BLAST search in the two *Physcomitrella* databases (www.cosmoss.org; http://moss.nibb.ac.jp).

Full-length cDNA clones were obtained from RIKEN Bioresource Centre, 3-1-1 Koyadai, Tsukuba, Ibaraki 305-0074, Japan (Nishiyama et al., 2003). *PpMdhar1* (pdp34716 (*1a*), pdp21517 (*1b*) and pdp17834 (*1c*)), *PpMdhar2* (pdp38825 (*2a*), pdp01778 (*2b*) and pdp33985 (*2c*)) and *PpMdhar3* (pdp26665 (*3a*), pdp37441 (*3b*), pdp04463 (*3c*), pdp45399 (*3d*) and pdp40062 (*3e*)). To obtain the 5' UTR from genomic DNA reverse primers specific to the coding region and forward primers specific to the 5' end of the different cDNA clones were used. The reverse primers were *PpMdhar1* (5' ACCACTGCTTCATCTCCCTTGC), *PpMdhar2* (5' GAATTTGTGAGCCTGAATCGTTGG) and *PpMdhar3* (5' GCATCAGCTCCAGGAGTCTTG). The forward primers were *PpMdhar1a* (5' TCGAGCTCTTACACGGTGAGTCC), *-1b* (5' GTCTGTGAGCCGATGCTCTGC), *-1c* (5' TACGTGTCCGCCTGATTTAGTTGC), *-2a* and *-2b* (5' GAATTTGTGAGCCTGAATCGTTGG), *-b3* (5' GTGCCGATTTAAACACTCGATCCAG), *-3a* and *-3b* (5' GCCGTTTGCCCTCCTCGTTG), *-3c* (5'-CAAACTAGCTCTCCTCCGGGCTC), *-3d* and *-3e* (5' TAGTGTCGGACTCTCGTACGGG). The full length coding region of the three MDHAR isoforms was obtained by standard PCR using the following primer sets; *PpMdhar1* (5' TACGTGTCCGCCTGATTTAGTTGC; 5' GCACACAACACAGGCTCTTCAG), *PpMdhar2* (5' CGCTGTAGAAGGTGACGTTAT; 5' GACGAGAAACGCACCACCAA) and *PpMdhar3* (5' TAGTGTCGGACTCTCGTACGGG; 5' AAACAAGTCGTGTGGATTAGCTAG). The PCR product was cloned into the pGEM-Teasy vector (Promega) or PCR®8/GW/TOPO® (Invitrogen) and sequenced. PCR reactions were carried out using Elongase Enzyme Mix (Invitrogen). All sequencing reactions were performed using BigDye® Terminator v3.1 Cycle Sequencing Kit (Applied Biosystems). The sequences were deposited at GenBank under accession number DQ159869 (*PpMdhar1*), DQ159870 (*PpMdhar2*) and DQ159871 (*PpMdhar3*).

RNA extraction, cDNA synthesis and quantitative real-time RT-PCR (qRT-PCR)

Total RNA was extracted from protonema or gametophytes using TRIzol (Invitrogen) according to the manufacturer's instructions. Purified RNA was treated with DNaseI using the DNA-free kit (Ambion, USA). RNA integrity was checked on a 1% (w/v) agarose gel containing ethidium bromide. The cDNA was synthesised using SuperScript™ III First-Strand Synthesis System (Invitrogen) and 2.5 µM oligo-dT (18-20) primer according to manufactures protocol. The qRT-PCR analysis was performed essentially as described in Burton et al. (2004). Four control genes were used in each experiment. The *Physcomitrella* sequences for the control genes were identified by a BLAST search using the *Arabidopsis* sequences for *histone3* (BT003326), *elongation factor 1-α* (P13905), *actin2* (NP_188508) and *tubulin β-1* (NP_177706) against the *Physcomitrella* transcriptome (http://www.cosmoss.org). The following contigs; *His3* (PPP_10973_C1), *eF1α* (PPP_395_C9), *Act2* (PPP_sd_37-C2) and *Tub1* (PPP_sd_36_C6) were obtained and primers were designed to the 3' end of the sequences (Table 1). Primers specific to *PpMdhar1*, *PpMdhar2* and *PpMdhar3* were designed using a forward primer specific to the coding region and a reverse primer specific to the 3' UTR (Table 1). To determine changes in alternative splicing of *PpMdhar3* five reverse primers were designed to anneal only to a specific splice variant. Each primer-set was tested against all other splice variants to ensure specificity before being used for qRT-PCR. The same forward primers were used in all experiments allowing the relative level of each splice product be determined (Table 1). *Insert table 1*

Genomic DNA purification, Southern blotting, genomic walking and promoter analyses

Genomic DNA was purified as in Schlink and Reski (2002). Southern blotting was performed by digesting 10 µg DNA with DraIII or SpeI and blotting it on to Hybond N^+ (Amersham Biosciences). The probes used for hybridisation were generated by PCR using primers specific to the 5' and 3' end of the 324/321 bp exon and EST clone pdp34716 (*PpMdhar1*), pdp38825 (*PpMdhar2*) and pdp26665 (*PpMdhar3*) as template. The following primers were used;

PpMdhar1 (5'GGCGAAGTCGTGGACGAGTACG; 5'GCACACAACACAGGCTCTTCAG), *PpMdhar2* (5'GGCGAAGTCGTGGACGAGTACG; 5'GACGAGAAACGCACCACCAA) and *PpMdhar3* (5'AAACAAGTCGTGTGGATTAGCTAG; 5'GACGACTACGACTACCTGCCC). The probe was labelled with α-[^{32}P]-dCTP using Rediprime^{TM} II (Amersham Biosciences) according to manufactures directions. The promoter sequences were obtained by genomic walking as described in Siebert et al. (1995). Genomic DNA (15 μg) was digested over night with 100 U of DraI, NruI, HpaI, StuI, SmaI, EcoRI, HincII or PvuII, phenol/chloroform purified and ligated to a 5' adaptor to generate eight different templates. The 5' sequences were obtained by nested PCR using gene specific and adaptor specific primers. All PCRs were performed using *Taq* DNA polymerase (Qiagen). The overlapping sequences obtained from the 8 templates were aligned using Contig Express (Vector NTI 8). The promoter sequence was analysed using NSITE-PL (www.softberry.com), PLACE (http://www.dna.affrc.go.jp/PLACE) and PlantCARE (http://intra.psb.ugent.be:8080/PlantCARE/).

Phylogenetic analysis

The MDHAR protein sequence of *Tortula ruralis* and the chloroplastic MDHAR sequences of *Hordeum vulgare* and *Medicago truncatula* were deduced from assembled EST sequences. For the phylogenetic analysis, only those monocotyledonous and dicotyledonous species that appeared to have a full complement of MDHAR sequences were chosen. MDHAR sequences were retrieved from GenBank, TIGR* (www.tigr.org) or from the Dow Joint Genome Institute's website+ (http://www.jgi.doe.gov/) the accession number being AtMDHAR1 (NP_190856), AtMDHAR2 (NP_568125), AtMDHAR3 (NP_566361), AtMDHAR4 (NP_189420), AtMDHAR5 (NP_564818), OsMDHAR1 (BAD46251.1), OsMDHAR2 (XP_483751.1), OsMDHAR3 (XP_467388.1), OsMDHAR4 (XP_467387.1), OsMDHAR5 (XP_480126.1), PtMDHAR1 (estExt_Genewise1_v1.C_281071+), PtMDHAR2 (estExt_Genewise1_v1.C_LG_I2528+),

PtMDHAR3 (grail3.0008044801[+]), MtMDHAR1 (TC100873*), MtMDHAR2 (TC101912*), MtMDHAR3 (TC96552,* TC109665*), GsMDHAR1 (TC32266*), GsMDHAR2 (TC32810*), GsMDHAR3 (TC28826*), GsMDHAR4 (TC28940*), TaMDHAR1 (TC206115*), TaMDHAR2 (TC220424*), TaMDHAR3 (BT009417), TaMDHAR4 (TC203466*), ZmMDHAR1 (AY103967), ZmMDHAR2 (AY107597), ZmMDHAR3 (AY106646), ZmMDHAR4 (TC249772*), HvMDHAR1 (TC139665*), HvMDHAR2 (TC139584*), HvMDHAR3 (TC139863*), HvMDHAR4 (Assembled from Unigene Hv.9974), PinMDHAR1 (TC42361*), PinMDHAR2 (TC45378*, BQ198625), TrMDHAR1 (Assembled from ESTs), CerMDHAR2 (BE642581). Three incomplete sequences (PinMDHAR2, MtMDHAR3, GsMDHAR4) from the chloroplast/mitochondrial targeted subfamily were included to increase the number and diversity of sequences. The selected sequences were aligned using the ClustalW software package (Chenna et al., 2003). Phylogenetic analyses were carried out by using various programs of the Phylogenetic Interference Package (PHYLIP) 3.63 (http://evolution.genetics.washington.edu/phylip.html). Protein distance matrices were calculated with PROTDIST using the PMB model (Veerassamy et al., 2003). A Gamma distributed rate of evolution across the amino acid positions was assumed with the shape parameter $\alpha = 0.91$ that had been calculated from the data by TREE-PUZZLE (Schmidt et al., 2002). Trees were generated with WEIGHBOR (Bruno et al., 2000) and TreeView (Page, 1996). To estimate the confidence limits of nodes 200 bootstrap samples were generated with SEQBOOT and the majority rule consensus tree was generated by CONSENSE.

Results

Gene structure of PpMdhar genes.

To identify members of the MDHAR gene family in *Physcomitrella patens,* a BLAST search was performed in the *Physcomitrella* EST databases (Lang et al., 2005; Nishiyama et al., 2003). The majority of the EST sequences deposited in the databases have been generated from high quality libraries containing mainly full length cDNAs (Nishiyama et al., 2003). The five MDHARs identified in *Arabidopsis* were used as query sequences. The search revealed the presence of 41 ESTs covering the 5' end, 43 ESTs covering the 3' end and nine ESTs corresponding to the central region of the full length cDNA. When sequences with more than 99% identity over a stretch of 200 bp were grouped together, the EST sequences from the 3' end generated three contigs. In contrast, when the EST sequences from the 5' ends were assembled using the same criteria, 11 contigs were generated. The differences in the sequences from the 5' end were all found in the 5' UTR upstream of the start ATG. The cDNA clones representing each of the 11 different contigs were obtained through RIKEN and nucleotide sequence analysis showed that the coding region gave rise to 3 enzyme isoforms, which we have designated PpMDHAR1 (434 aa), PpMDHAR2 (433 aa) and PpMDHAR3 (434 aa). The cDNAs encoding *PpMdhar1*, *PpMdhar2* and *PpMdhar3* had three, three and five different 5' UTRs, respectively. To resolve whether the differences in the 5' UTR resulted from mRNAs originating from different genes or from alternative splicing, the genomic DNA fragments were obtained by PCR using reverse primers specific to the 5' end of each of the ESTs. Direct sequencing of the PCR products revealed that each of the 5' UTRs originated from the same genomic sequence and could be created by alternative splicing of a long mRNA leader sequence of 749-1100 bp (Fig. 1A). When the genomic sequences of the *PpMdhar1* and *PpMdhar2* 5' UTRs were aligned, the sequences showed a high level of similarity ($P<4*10^{-12}$; PRSS3). No significant similarity was found between the 5' UTRs of *PpMdhar1* and *PpMdhar3* and

PpMdhar2 and *PpMdhar3*, respectively. Southern blotting using a probe specific to the last 300 nucleotides of the coding region of *PpMdhar1*, *PpMdhar2* or *PpMdhar3* confirmed that only one copy of each gene was present in the genome (Fig. 1B). To test for specificity and lack of cross hybridisation, control plasmids carrying the three genes were included (not shown). *Insert figure 1*

The number of preAUGs and the free energy of the secondary folding of the 5' UTR was determined using *m*fold 3.1 (Table 2) (Zuker, 2003). All the splice variants of the *PpMdhar3* had a considerably lower ΔG than those of *PpMdhar1* and *PpMdhar2*, but up to two fold differences in the calculated free energy were also found between splice variants from the same gene as seen with *PpMdhar3a* and *PpMdhar3c* and *PpMdhar2b* and *PpMdhar2c* (Table 2). The differences in ΔG and presence of preAUGs is likely to result in a much lower rate of translation from e.g. the *PpMdhar3a*, *PpMdhar3b, PpMdhar3d, PpMdhar3e* compared to *PpMdhar3c* (Kawaguchi and Bailey-Serres, 2005). Although several preAUGs are present, none of them generated a MDHAR isoform with a NH_2-terminal extension. *Insert table 2*

Phylogenetic analysis of MDHAR

An alignment of the available MDHAR protein sequences from plants show a high level of identity and complete conservation of the FAD/NAD-binding sites. The sequences can be divided into three subfamilies consisting of cytosolic isoforms (433-436 aa), peroxisomal isoforms having a COOH-terminal extension (476-488 aa) and chloroplast/mitochondrial isoforms having an NH_2-terminal extension (483-497 aa). The NH_2-terminal extension has been shown to act as a transit peptide for mitochondrial or chloroplast targeting in rice and *Arabidopsis* (Obara et al., 2002; Chew et al., 2003; Obara and Fukuda, 2004). The COOH-terminal extension contains the targeting sequence to the peroxisomal membrane and is predicted to be a transmembrane helix which acts as a membrane anchor (Lisenbee et al., 2005). Except for the terminal extensions, no major gaps were found in the protein alignment.

Using 35 full-length and three partial MDHAR sequences, a neighbour-joining tree was constructed (Fig. 2A). Three partial sequences for chloroplast/mitochondrial MDHAR isoforms were included to ensure that evolutionarily distant plants were represented. Including these sequences did not cause any distortion of the tree. To maintain clarity, sequences from angiosperms were only included from species where more than two MDHAR sequences were available. The phylogenetic tree generates three main clades which are well supported by high bootstrap values (Fig 2A). In a previous study, including only sequences from angiosperms the same three main clades were identified (Sano et al., 2005). The single MDHAR gene found in algae forms the base of the tree. The main clades represent MDHAR isoforms located to the same subcellular compartment and show that each subfamily is likely to be of monophyletic origin. Within each main clade, the topology reflects the taxonomic classification of plants. In the chloroplast/mitochondrial and the peroxisomal clade, each plant species is only represented once, with the exception of GsMDHAR2 and GsMDHAR3 from *Gossypium* and OsMDHAR3 and OsMDHAR4 from *Oryza sativa*. In contrast, 2-3 paralogues from each species are represented in the cytosolic clade. The three MDHARs from *Physcomitrella,* together with the MDHAR from the moss *Tortula ruralis*, form a separate well supported cluster within cytosolic MDHARs.

Although not included in the tree, a short partial EST sequence from fern was also identified which contained a unique amino acid insertion present only in chloroplast/mitochondrial MDHARs (Fig 2B). *Insert figure 2*

The gene structures for the three *Mdhar* subfamilies from angiosperms show distinct differences in intron-exon structure. The cytosolic and membrane-bound peroxisomal subfamily contains introns at conserved positions within the coding region, the difference being that intron 1, 8 and 9 are absent and the terminal exon has been extended by 126-165 nucleotides in the peroxisomal subfamily (Fig. 3). In contrast, the chloroplast/mitochondrial subfamily has a completely different intron-exon structure and none of the intron positions are identical to the intron

positions in the chloroplast/mitochondrial subfamily. To further investigate the evolutionary relationship between *PpMdhar1*, *PpMdhar2* and *PpMdhar3* and the *Mdhar genes* from higher plants, the coding region was cloned from genomic DNA of *Physcomitrella* and the sequence aligned with the cDNA sequence. All three genes showed an exon-intron structure similar to the cytosolic MDHARs, confirming that the *PpMdhar* genes share a common ancestor with the genes encoding the cytosolic MDHARs from higher plants (Fig. 3). *Insert figure 3*

Regulation of PpMdhar expression

Since *Physcomitrella* expresses three putative cytosolic PpMDHARs, it was important to determine if they had different functional roles. We therefore analysed whether they were differentially expressed in different tissue types or under different stress conditions. The majority of the ≈100,000 *Physcomitrella* ESTs in the public databases are derived from 8-14 day old untreated tissue or tissue exposed to cytokinin or auxin (Nishiyama et al., 2003). ESTs representing *PpMdhar1*, *PpMdhar2* and *PpMdhar3* were identified in all three libraries and there were no significant differences in the representation of the genes in the libraries. To determine if there were developmental changes in the expression of *PpMdhar1*, *PpMdhar2* and *PpMdhar3*, quantitative real time RT-PCR (qRT-PCR) was performed on *Physcomitrella* tissue from 1 week old protonema tissue and 5 week old gametophytes. For *PpMdhar2* and *PpMdhar3* the transcription levels were identical in the two developmental stages while for *PpMdhar1*, a 50% higher level of transcript was observed in the gametophytes (Fig. 4B; $P<0.05$). *Insert figure 4*

To analyse if the expression of the *PpMdhar* genes changes under abiotic stress, 1 week old protonema were exposed to oxidative, salt, osmotic, cold or UV-B stress. A treatment with abscisic acid (ABA) was also included. For *PpMdhar1*, an increase in transcript level was observed after two hours of treatment with salt or ABA. After 4 hours, the maximal 4-fold induction was attained (Fig. 5A). The PEG treatment elicited a similar response to 60 mM NaCl indicating that the

upregulation is a response to water loss rather than to salt toxicity, since the osmotic potential was similar under the two treatments. Exposure to cold, UV-B radiation or methyl viologen (MeV) did not affect the expression of *PpMdhar1* (Fig. 5A). The expression of *PpMdhar3* was also upregulated 5-fold upon ABA treatment and again the highest level of expression was measured 4 hours after initiation of the treatment (Fig. 5C). The expression level of *PpMdhar3* also increased under salt and osmotic stress and the timing of the response was identical to *PpMdhar1*. In contrast, *PpMdhar2* transcript levels were essentially unchanged after exposure to the same range of abiotic stresses (Fig. 5B). *Insert figure 5*

None of the genes showed significant upregulation under oxidative stress following treatment with 100 μM MeV (Fig. 5). Protonema was subsequently exposed to 50, 100 or 200 μM MeV and time points taken every 24 h for 5 days, to ensure that a potential induction at a later time point was not missed or that the concentration of MeV had not been too high or too low. At 200 μM MeV, the tissue started to show signs of bleaching after 1-2 weeks. None of *PpMdhars* was induced under these conditions (not shown). At 50 μM MeV, no visual oxidative damage was apparent within the time frame of the experiment.

Because of the extensive alternative splicing of the 5' UTR, we wanted to determine if there was an extra point of regulation at the level of translation. *PpMdhar3a* and *-3b* are the major transcripts and represent 36 and 59% of the *PpMdhar3* mRNA population, respectively, whereas only 1% has the additional 77 bp removed (Fig. 1). The two splice variants *PpMdhar3d* and *-3e* represents 1 and 3% of the total *PpMdhar3b* mRNA, respectively. No change in the relative level of the five *PpMdhar3* splice forms was detected and the level of all splice variants increased upon ABA treatment and under salt stress and was unchanged under cold and oxidative stress (Fig. 6A-E). To determine whether the developmental stage of *Physcomitrella* affected the splicing of the 5' UTR, qRT-PCR was done on cDNA from protonema and gametophytes. No difference was found in the level of *PpMdhar3a*, *PpMdhar3b* and *PpMdhar3c*, however, a 2.1±0.4 fold increase was

observed for *PpMdhar3d* and *PpMdhar3e* (P<0.004) in the gametophyte compared to protonema. This change is most likely not a difference in the splicing pattern, but reflects that more transcripts are initiated at the second transcription start site in the gametophyte (see below). *Insert figure 6*

In silico promoter analysis

The promoter sequences upstream of *PpMdhar1*, *PpMdhar2* and *PpMdhar3* were obtained by genomic walking. For each *PpMdhar* gene, more than 1,000 bp were obtained 5' of the start of transcription. For the *PpMdhar1* and *PpMdhar3* promoter, a putative TATA-box was identified at -157 bp and -106 bp, respectively, but no TATA-box could be identified in the *PpMdhar2* promoter. The majority of the EST sequences are obtained from a high quality library containing mainly full length cDNA clones (Nishiyama et al., 2003). The two putative TATA-boxes in *PpMdhar1* and *-3* are more than 100 bp away from the start of the cDNA clones and it is therefore likely that none of the three genes utilise a TATA-box for transcription initiation. A recent estimate for *Arabidopsis* suggests that only 29% of all genes utilise a TATA-box (Molina and Grotewold, 2005). The difference in transcript length between *PpMdhar3a*, *PpMdhar3b*, *PpMdhar3c* and *PpMdhar3d* and *PpMdhar3e*, respectively, suggest that there could be two transcription start sites in the *PpMdhar3* promoter (Fig. 1). In the following analysis, the 5' end of the beginning of the longest cDNA clones is therefore used as reference point.

A member of the bHLH transcription factor family was located 5' to the *PpMdhar1* and *PpMdhar2* genes at -737 bp (Acc nr. AW155883) and -774 bp (Acc nr. BJ581653), respectively. The significant similarity of the 5' UTRs and the presence of a gene from the same family 5' of *PpMdhar1* and *PpMdhar2*, suggest that these two genes have evolved by a recent duplication of a portion of the chromosome. Since the two genes respond differentially when exposed to ABA, *PpMdhar1* being up-regulated and *PpMdhar2* transcription level remains unchanged, the promoter region was analysed for putative *cis*-elements that could be responsible for this difference. An *in*

silico analysis was done on 250 bp upstream of the transcription start site of *PpMdhar1, PpMdhar2* and *PpMdhar3* (Higo et al., 1999; Lescot et al., 2002). An exact match to the strong ABRE consensus sequence GCCACGT(C/G) was found in the *PpMdhar1* promoter at position -132 ($P<0.05$; Fig. 7; Zhu, 2002). In addition, a weaker match was identified at position -45 (ACCACGTT, mismatches underlined). The specificity of the ABRE element is determined both by the sequence surrounding the core ACGT and by its association with coupling elements (Yamaguchi-Shinozaki and Shinozaki, 2005). An ABA-specific coupling element CE3 was identified close to the initiation site for transcription at -74 of *PpMdhar1* (CGCGTGCC) (Shen et al., 2004). When the sequence surrounding these elements was aligned with the homologous sequences from *PpMdhar2*, only the weakly matching ABRE element at position -84 (equivalent to position -45 in *PpMdhar1*) was conserved. Neither the ABRE element at position -170 nor the CE3 element at position -113 was conserved in the *PpMdhar2* promoter (Fig. 7). No other putative ABRE elements could be identified in the *PpMdhar2* promoter. In the *PpMdhar3* promoter, an ABRE element (GGGGGACGT) was also identified near the putative transcription initiation site at -23 bp. A core sequence of an ABA coupling element CE1 was identified at -225 bp (CCACC; Shen et al., 2004). *Insert figure 7*

Discussion

Most studies on plant adaptation to environmental stress have been conducted within a few model species or in plants adapted particularly well to a certain stress. The identification of stress related genes in the ancient non-vascular *Physcomitrella* can fill the gap between studies in algae and in vascular plants and provide information on the evolution of plant responses to abiotic stress.

We have identified three genes, *PpMdhar1*, *PpMdhar2* and *PpMdhar3* encoding monodehydroascorbate reductase in *Physcomitrella*. All three genes resemble the cytosolic MDHARs from higher plants in having neither the NH_4-terminal nor the COOH-terminal extension found in chloroplast/mitochondrial or membrane-bound peroxisomal MDHAR, respectively (Fig 2A; Fig 3; Sano et al., 2005).

The function of the cytosolic ascorbate-glutathione pathway is largely unknown, but the conservation of this gene family implies that cytosolic MDHAR plays a central role in plants in the defence against ROS. A recent study of an *Arabidopsis* mutant lacking cytosolic ascorbate peroxidase, Apx1, showed that the mutant plant had high levels of H_2O_2 and protein oxidation even in the chloroplast upon exposure to high light stress (Davletova et al., 2005). Surprisingly, the absence of ascorbate peroxidase in the cytosol proved more severe than the absence of the stroma targeted ascorbate peroxidase. Hence, cross-compartment protection occurs and together with SOD and APX, cytosolic MDHAR is likely to play an important role protecting the whole plant during abiotic stress. It is possible that the acquisition of a cytosolic ascorbate-glutathione pathway was advantageous when the first plants colonised the more challenging terrestrial environment. In *Chlamydomonas*, ascorbate peroxidase and MDHAR activity has only been detected in the chloroplast and not in the cytosol (Takeda et al., 1997).

Evolution of MDHAR in plants

The identification of three MDHAR homologues in *Physcomitrella* allowed a thorough phylogenetic study of the MDHAR gene family including sequences from algae, non-vascular and vascular plants. The chloroplast/mitochondrial, membrane-bound peroxisomal and cytosolic MDHARs fall in separate phylogenetic clades, suggesting that two major duplication and diversification events gave rise to these subfamilies (Fig. 2A). The differences in amino acid sequence and intron-exon structure indicate that the chloroplast/mitochondrial MDHARs diverged early in evolution and that the membrane-bound peroxisomal MDHARs evolved by a more recent duplication. The apparent absence of a chloroplast/mitochondrial targeted MDHAR in *Physcomitrella* could imply that the first duplication occurred after the divergence of bryophytes. However, the completely different intron-exon boundaries in the chloroplast/mitochondrial and cytosolic/peroxisomal MDHARs show that the ancestral gene was a more compact gene lacking introns. The duplication must therefore have occurred before the divergence of bryophytes, since the three *PpMdhars* already contain introns at conserved positions.

Because of the low availability of ESTs and genome sequences from seedless vascular plants, it is not yet possible to determine exactly when the second duplication generating the peroxisomal subfamily occurred. No ESTs encoding the membrane-bound peroxisomal MDHAR were identified in moss (~100.000), fern (~3.500) or pine EST (~191.000) databases. This could imply that the second duplication generating the ancestor of the membrane-bound peroxisomal MDHAR occurred after the divergence of the gymnosperms. Unfortunately, biochemical studies on the cellular location of MDHAR activity have so far not been performed on other plants than angiosperms. A cytosolic MDHAR from *Arabidopsis* (AtMDHAR1) was recently shown to be inefficiently targeted from the cytosol to the peroxisomal matrix (Lisenbee et al., 2005). The three terminal amino acids in PinMDHAR1 (-SKI), PpMDHAR1 (-SKI), PpMDHAR2 (-SKV) and PpMDHAR3 (-AKI) show some resemblance to the peroxisomal matrix consensus targeting

sequence (-SKL) and it is possible that a partial localisation of cytosolic MDHAR to the peroxisome is sufficient to maintain ascorbate recycling in this organelle in non-angiosperms.

Within the cytosolic clade, the four MDHARs from bryophytes are separated in their own group. This implies that although both *Physcomitrella* and *Arabidopsis* contain three cytosolic MDHARs, they are not orthologs with a conserved function. Instead it appears that gene duplications have occurred after diversification and speciation.

A recent phylogenetic analysis of the ascorbate peroxidase family from rice and *Arabidopsis* showed that the chloroplast and non-chloroplast targeted ascorbate peroxidases had a completely different intron-exon structure and unique amino acid signatures were identified in the chloroplast/mitochondrial subfamily (Teixeira et al., 2004). In contrast, the peroxisomal and cytosolic ascorbate peroxidase subfamilies had essentially conserved intron positions except that the two terminal exons were fused and extended in the genes encoding the peroxisomal enzymes. Based on the similarities in gene structure between the three MDHAR subfamilies (Fig 3) and the ascorbate peroxidases, one could speculate that the two gene families have followed a similar evolutionary path with respect to major duplication and diversification events. In the liverwort *Marchantia paleacea*, a cytosolic CuZn-SOD showing higher similarity with the chloroplast targeted CuZn-SODs from vascular plants, but lacking the transit peptide has been identified (Tanaka et al., 1998). This suggest that the duplication and diversification of CuZn-SOD occurred before the divergence of bryophytes. As more sequences from bryophytes and seedless vascular plants become available it will be possible to further explore the possibility of co-evolution of the enzymes of the ascorbate-glutathione pathway.

Is MDHAR absent in Physcomitrella chloroplast and mitochondria?

The ascorbate-glutathione pathway has been studied in most detail in the chloroplast. The lack of ESTs representing the chloroplast/mitochondrial MDHAR in *Physcomitrella* raises an

important question: Do bryophytes lack the complete ascorbate-glutathione pathway in these ROS producing organelles? In *Arabidopsis*, the chloroplast targeted and the cytosolic MDHARs are represented by approximately the same number of ESTs in the TIGR database. Furthermore, in the fern *Ceratopteris richardii* an EST containing the amino acid signature of a chloroplast targeted MDHAR was identified amongst a total 3,587 ESTs (Fig. 2B). Although the *Physcomitrella* EST collection contains >100,000 sequences, the possibility that a chloroplast/mitochondrial MDHAR is transcribed at very low levels and therefore not represented in the EST collection can not be excluded. However, it does appear that *Physcomitrella* only contains the cytosolic versions of MDHAR. A BLAST search for other members of the ascorbate-glutathione pathway reveals that putative chloroplastic versions of APX, SOD and DHAR can be identified. In higher plants, chloroplast targeted APX are found in both the stroma and bound to the thylakoid membrane. However, only the thylakoid-membrane bound version could be identified in the *Physcomitrella* EST database. Chloroplast SODs are either Fe-SOD or CuZn-SOD and only ESTs for the former SOD with a putative transit peptide were identified in moss. Fe-SOD is generally not highly expressed in vascular plants, hence, scavenging of ROS in moss chloroplast could rely on a different set of enzymes. It has been shown that ferredoxin is highly efficient in reducing monodehydroascorbate near the thylakoid membrane and, thus moss could be more dependent on this alternative pathway (Asada, 1999). A putative chloroplast targeted DHAR was identified in *Physcomitrella* and moss could rely more on this enzyme or other enzymes with DHAR activity e.g. thioredoxins and glutathione peroxidases for the reduction of dehydroascorbate and hence monodehydroascorbate (Arrigoni and Tullio, 2002). The apparent differences in enzyme composition did not cause high sensitivity to oxidative stress, as *Physcomitrella* could be exposed to high level of MeV without showing immediate signs of bleaching (not shown).

PpMdhar1 and PpMdhar3 are upregulated under water stress

Expression studies in a variety of plant species have shown that both cytosolic and chloroplast/mitochondrial MDHAR is upregulated during a range of stresses including salt, drought, oxidative stress and cold (Ozturk et al., 2002; Rizhsky et al., 2002; Baek and Skinner, 2003; Hernandez et al., 2003; Yoon et al., 2004). Two out of the three *PpMdhars* showed increased expression after protonema had been exposed to salt or osmotic stress. When salt and PEG levels were adjusted to the same osmotic potential, a similar increase in transcription was observed. It is therefore likely that the upregulation of *PpMdhar1* and *PpMdhar3* is a response to low turgor rather than salt toxicity. The sensor of low turgor has not yet been identified in plants, but it is known that loss of turgor is associated with ABA accumulation. The increased expression of *PpMdhar1* and *PpMdhar3* when protonema was exposed to exogenous added ABA suggest that the two genes are regulated by increased ABA levels and that ABA-independent regulatory pathways are not required. It has been suggested that late responsive genes involved in the removal of ROS are not responding to the initial loss in turgor but rather to the secondary damage done by the stress (Zhu, 2002). The lack of upregulation of *PpMdhar1* and *PpMdhar3* after treatment with MeV or UV-B, clearly shows that oxidative damage per se does not act as signal to increase *Mdhar* transcription in *Physcomitrella*. This is in contrast to higher plants where treatment with high levels of MeV (~2 mM) lead to a brief 1.3-1.6 fold upregulation of a putative cytosolic MDHAR from *Brassica campestris* (Yoon et al., 2004).

In *Arabidopsis* the three cytosolic MDHARs were differentially expressed when plants were exposed to a range of abiotic stresses. *AtMdhar1* was upregulated under drought, salt, cold and high light stress, *AtMdhar2* under drought and high light stress, whereas *AtMdhar3* expression decreased under stress (Mittler et al., 2004). The phylogenetic analysis, however, showed that the cytosolic *AtMdhars* and *PpMdhars* are not orthologs and the differential expression in *Physcomitrella* and *Arabidopsis* has been evolved more than once during the evolution of plants. The high similarity

between the *PpMdhar1* and *PpMdhar2* genes suggest that the generation of an ABA-responsive and a non-responsive *Mdhar* is an evolutionarily relatively recent event in *Physcomitrella*.

The promoter regions of *PpMdhar1*, *PpMdhar2* and *PpMdhar3* were obtained by genomic walking and analysed for ABRE regulatory elements. The consensus sequence used for the *in silico* analysis is based on ABRE elements from vascular plants, but these elements appear to be highly conserved and serve a similar function in *Physcomitrella*. It has previously been shown that a wheat promoter containing an ABRE-element was upregulated in *Physcomitrella* when protoplasts were exposed to ABA or osmotic stress (Knight et al., 1995). Since *PpMdhar1* and *PpMdhar2* have originated from a more recent duplication it was possible to compare the presence or absence of regulatory elements in these two promoters. The presence of a perfect match to the strong ABRE element and a putative coupling element in the *PpMdhar1* promoter which was not conserved in the *PpMdhar2* promoter indicates that these two elements are involved in the ABA dependent regulation. Although we do not know which transcription factor is involved in the ABA-dependent upregulation, a bZIP factor (ABI3) was recently identified and shown to be upregulated after 4h of dehydration in *Physcomitrella* (Frank et al., 2005). The bZIP factor is known to bind ABRE elements and upregulate stress response genes in higher plants (Zhu, 2002).

Since all three *PpMdhar* genes undergo alternative splicing of the 5' UTR, we wanted to determine if the splicing acted as an extra level of regulation under abiotic stress. In *Arabidopsis*, a 5' UTR longer than 175 bp or a ΔG below -55 kcal/mol had a negative effect on ribosomal loading and thus on translation efficiency (Table 2) (Kawaguchi and Bailey-Serres, 2005). However, no change was observed in the relative contribution from the splice forms and when the *PpMdhar3* transcript increased under osmotic stress the contribution from all splice forms increased (Fig. 6). It is therefore unlikely, that the alternative splicing plays an additional regulatory role under the abiotic stresses tested in this paper. Alternative splicing of the 5' UTR has also been shown to be

involved in regulation of tissue or cell specific expression, but no difference in 5' UTR splicing pattern was observed between protonema and mature gametophytes.

In summery, the data reported in this work show that cytosolic MDHAR plays an important role in both vascular and non-vascular plants. The upregulation of two *PpMdhar* genes upon exposure to water deficiency suggests that ROS scavenging in the cytosol is particular important upon dehydration. The apparent absence of organelle targeted MDHAR in *Physcomitrella* deserves further attention. The ongoing sequencing of the *Physcomitrella* genome will allow further investigation of the loss or gain of ROS scavenging enzymes during the evolution of land plants.

Acknowledgement

Christina Lunde was funded by the Danish Agricultural and Veterinary Research Council.

The cDNA clones encoding *PpMdhar* were obtained through RIKEN, Japan.

References

Arrigoni, O., Dipierro, S. and Borraccino, G. 1981. Ascorbate free-radical reductase, a key enzyme of the ascorbic-acid system. FEBS lett 125: 242-244

Arrigoni, O. and Tullio, D.M.C. 2002. Ascorbic acid: much more than just an antioxidant. Biochim Biophys Acta 1569: 1-9

Asada, K. 1999. The water-water cycle in chloroplasts: Scavenging of active oxygens and dissipation of excess photons. Annu Rev Plant Physiol Plant Mol Biol 50: 601-639

Ashton, N.W. and Cove D.J. 1977. Isolation and preliminary characterization of auxotrophic and analog resistant mutants of moss, *Physcomitrella patens*. Mol Gen Genet 154: 87-95

Ashton, N.W., Grimsley, N.H. and Cove, D.J. 1979. Analysis of gametophytic development in the moss *Physcomitrella patens* using auxin and cytokinin resistant mutants. Planta 144: 427-435

Baek, K.H. and Skinner, D.Z. 2003. Alteration of antioxidant enzyme gene expression during cold acclimation of near-isogenic wheat lines. Plant Sci 165: 1221-1227

Bérczi, A. and Møller, I.M. 1998. NADH-monodehydroascorbate oxidoreductase is one of the redox enzymes in spinach leaf plasma membranes. Plant Physiol 116: 1029-1036

Bruno, W.J., Socci, N.D. and Halpern, A.L. 2000. Weighted Neighbor Joining: A Likelihood-Based Approach to Distance-Based Phylogeny Reconstruction. Mol Biol Evol 17: 189-197

Burton, R.A., Shirley, N.J., King, B.J., Harvey, A.J. and Fincher, G.B. 2004. The CesA gene family of barley. Quantitative analysis of transcripts reveals two groups of co-expressed genes. Plant Physiol 134: 224-236

Chenna, R., Sugawara, H., Koike, T., Lopez, R., Gibson, T.J., Higgins, D.G. and Thompson, J.D. 2003. Multiple sequence alignment with the Clustal series of programs. Nucleic Acids Res 31: 3497-3500

Chew, O., Whelan, J. and Millar, A.H. 2003. Molecular definition of the ascorbate-glutathione cycle in *Arabidopsis* mitochondria reveals dual targeting of antioxidant defenses in plants J Biol Chem 278: 46869-46877

Dalton, D.A., Langeberg, L. and Robbins, M. 1992. Purification and characterization of monodehydroascorbate reductase from soybean root-nodules. Arch Biochem Biophys 292: 281-286

Dalton, D.A., Baird, L.M., Langeberg, L., Taugher, C.Y., Anyan, W.R., Vance, C.P. and Sarath, G. 1993. Subcellular-localization of oxygen defense enzymes in soybean (glycine-max [l] merr) root-nodules. Plant Physiol 102: 481-489

Davletova, S., Rizhsky, L., Liang, H.J., Zhong, S.Q., Oliver, D.J., Coutu, J., Shulaev, V., Schlauch, K. and Mittler, R. 2005. Cytosolic ascorbate peroxidase 1 is a central component of the reactive oxygen gene network of *Arabidopsis*. Plant Cell 17: 268-281

Frank, W., Ratnadewi, D. and Reski, R. 2005. *Physcomitrella patens* is highly tolerant against drought, salt and osmotic stress. Planta 220: 384-394

Hernandez, J.A., Aguilar, A.B., Portillo, B., Lopez-Gomez, E., Beneyto, J.M. and Garcia-Legaz, M.F. 2003. The effect of calcium on the antioxidant enzymes from salt-treated loquat and anger plants. Funct Plant Biol 30: 1127-1137

Higo, K., Ugawa, Y., Iwamoto, M. and Korenaga, T. 1999. Plant *cis*-acting regulatory DNA elements (PLACE) database. Nucleic Acid Res 27: 297–300

Hossain, M.A., Nakano, Y. and Asada, K. 1984. Monodehydroascorbate reductase in spinach-chloroplasts and its participation in regeneration of ascorbate for scavenging hydrogen-peroxide. Plant Cell Physiol 25: 385-395

Hossain, M.A. and Asada, K. 1985. Monodehydroascorbate reductase from cucumber is a flavin adenine-dinucleotide enzyme. J Biol Chem 260: 2920-2926

Kawaguchi, R. and Bailey-Serres, J. 2005. mRNA sequence features that contribute to translational regulation in *Arabidopsis*. Nucleic Acids Res 33: 955-965

Kenrick, P. and Crane, P.R. 1997. The origin and early evolution of plants on land. Nature 389: 33-39

Knight, C.D., Sehgal, A., Atwal, K., Wallace, J.C., Cove, D.J., Coates, D., Quatrano, R.S., Bahadur, S., Stockley, P.G.and Cuming, A.C. 1995. Molecular responses to abscisic-acid and stress are conserved between moss and cereals. Plant Cell 7: 499-506

Lang, D., Eisinger, J., Reski, R. and Rensing, S. 2005. Representation and high-quality annotation of the *Physcomitrella patens* transcriptome demonstrates a high proportion of proteins involved in metabolism among mosses. Plant Biol 7:238-250

Leonardis, D.S., Lorenzo, D.G., Borraccino, G. and Dipierro, S. 1995. A specific ascorbate free-radical reductase isozyme participates in the regeneration of ascorbate for scavenging toxic oxygen species in potato-tuber mitochondria. Plant Physiol 109: 847-851

Lescot, M., Déhais, P., Thijs, G., Marchal, K., Moreau, Y., van Peer, Y., Rouzé, P. and Rombauts, S. 2002. PlantCARE, a database of plant cis-acting regulatory elements and a portal to tools for in silico analysis of promoter sequences. Nucleic Acids Res 30:325-327.

Leterrier, M., Corpas, F.J., Barroso, J.B., Sandalio, L.M. and del Rio, L.A. 2005. Peroxisomal monodehydroascorbate reductase. Genomic clone characterization and functional analysis under environmental stress conditions. Plant Physiol 138 :2111-2123

Lisenbee, C.S., Lingard, M.J. and Trelease, R.N. 2005. Arabidopsis peroxisomes possess functionally redundant membrane and matrix isoforms of monodehydroascorbate reductase. Plant J 43: 900-914.

Mittler, R., Vanderauwera, S., Gollery, M. and van Breusegem, F. 2004. Reactive oxygen gene network of plants. Trends Plant Sci 9: 490-498

Mittova, V., Volokita, M., Guy, M. and Tal, M. 2000. Activities of SOD and the ascorbate-glutathione cycle enzymes in subcellular compartments in leaves and roots of the cultivated tomato and its wild salt-tolerant relative *Lycopersicon pennellii*. Physiol Plant 110: 42-51

Miyake, C. and Asada, K. 1994. Ferredoxin-dependent photoreduction of the monodehydroascorbate radical in spinach thylakoids. Plant Cell Physiol 35: 539-549

Molina, C. and Grotewold, E. 2005. Genome wide analysis of *Arabidopsis* core promoters BMC Genomics 6: doi:10.1186/1471-2164-6-25

Murthy, S.S. and Zilinskas, B.A. 1994. Molecular-cloning and characterization of a cDNA-encoding pea monodehydroascorbate reductase. J Biol Chem 269: 31129-31133

Nishiyama, T., Fujita, T., Shin-I, T., Seki, M., Nishide, H., Uchiyama, I., Kamiya, A., Carninci, P., Hayashizaki, Y., Shinozaki, K., Kohara, Y. and Hasebe, M. 2003. Comparative genomics of Physcomitrella patens gametophytic transcriptome and *Arabidopsis thaliana*: Implication for land plant evolution. Proc Natl Acad Sci USA 100: 8007-8012

Obara, K., Sumi, K. and Fukuda, H. 2002. The use of multiple transcription starts causes the dual targeting of *Arabidopsis* putative monodehydroascorbate reductase to both mitochondria and chloroplasts. Plant Cell Physiol 43: 697-705

Obara, K. and Fukuda, H. 2004. Alternative splicing of rice monodehydroascorbate reductase (MDAR) and its dual-targeting to mitochondria (Mt) and plastids (Pl). Plant Cell Physiol 45: S167-S167

Ozturk, Z.N., Talame, V., Deyholos, M., Michalowski, C.B., Galbraith, D.W., Gozukirmizi, N., Tuberosa, R. and Bohnert, H.J. 2002. Monitoring large-scale changes in transcript abundance in drought- and salt-stressed barley. Plant Mol Biol 48: 551-573

Page, R.D.M. 1996. TreeView: An application to display phylogenetic trees on personal computers. Comput Appl Biosci 12: 357-358

Polle, A. 2001. Dissecting the superoxide dismutase-ascorbate-glutathione-pathway in chloroplasts by metabolic modeling. Computer simulations as a step towards flux analysis. Plant Physiol 126: 445-462

Rizhsky, L., Liang, H.J. and Mittler, R. 2002. The combined effect of drought stress and heat shock on gene expression in tobacco. Plant Physiol 130: 1143-1151

Sano, S., Miyake, C., Mikami, B. and Asada, K. 1995. Molecular characterization of monodehydroascorbate radical reductase from cucumber highly expressed in *escherichia-coli*. J Biol Chem 270: 21354-21361

Sano, S., Tao, S., Endo, Y., Inaba, T., Hossain, M.A., Miyake, C., Matsuo, M., Aoki, H., Asada, K. and Saito, K. 2005. Purification and cDNA cloning of chloroplastic monodehydroascorbate reductase from spinach. Biosci Biotechnol Biochem 69: 762-772

Schlink, K. and Reski, R. 2002. Preparing high-quality DNA from moss. Plant Mol Biol Rep 20: 423a-423f

Schmidt, H.A., Strimmer, K., Vingron, M. and von Haeseler, A. 2002. TREE-PUZZLE: maximum likelihood phylogenetic analysis using quartets and parallel computing. Bioinformatics 18: 502-504

Shen, Q.X.J., Casaretto, J.A., Zhang, P. and Ho, T.H.D. 2004. Functional definition of ABA-response complexes: the promoter units necessary and sufficient for ABA induction of gene expression in barley (*Hordeum vulgare L.*). Plant Mol Biol 54: 111-124

Siebert, P.D., Chenchik, A., Kellogg, D.E., Lukyanov, K.A. and Lukyanov, S.A. 1995. An improved PCR method for walking in uncloned genomic DNA. Nucleic Acids Res 23: 1087-1088

Takeda, T., Ishikawa, T. and Shigeoka, S. 1997. Metabolism of hydrogen peroxide by the scavenging system in *Chlamydomonas reinhardtii*. Physiol Plant 99: 49-55

Tanaka, K., Takio, S., Yamamoto, I. and Satoh, T. 1998. Characterization of a cDNA encoding CuZn-superoxide dismutase from the liverwort *Marchantia paleacea var. diptera*. Plant Cell Physiol 39: 235-240

Teixeira, F.K., Menezes-Benavente, L., Margis, R. and Margis-Pinheiro, M. 2004. Analysis of the molecular evolutionary history of the ascorbate peroxidase gene family: Inferences from the rice genome. J Mol Evol 59: 761-770

Veerassamy, S., Smith, A. and Tillier, E.R.M. 2003. A transition probability model for amino acid substitutions from blocks. J Comput Biol 10: 997-1010

Yamaguchi-Shinozaki, K. and Shinozaki, K. 2005. Organization of *cis*-acting regulatory elements in osmotic- and cold-stress-responsive promoters. Trends Plant Sci 10: 88-94

Yoon, H.S., Lee, H., Lee, I.A., Kim, K.Y. and Jo, J.K. 2004. Molecular cloning of the monodehydroascorbate reductase gene from *Brassica campestris* and analysis of its mRNA level in response to oxidative stress. Biochim Biophys Acta 1658: 181-186

Zhu, J.K. 2002. Salt and drought stress signal transduction in plants. Annu Rev Plant Biol 53: 247-273

Zuker, M. 2003. *M*fold web server for nucleic acid folding and hybridization prediction. Nucleic Acids Res 31: 3406-3415

Tables

Table1. PCR primers and PCR product sizes in basepairs for the genes analysed

Gene/Splice variant	Forward Primer	Reverse Primer	PCR Size
β-tubulin-1	GAGTTCACGGAAGCGGAGAG	ATATCTTTCAGGCTCCACCG	224 bp
Elongation factor-1α	GCCAAGAAGAAGTGAATAGTGCG	ACGTCTGCCTCGCTCTAGC	166 bp
Actin 2	GCGAAGAGCGAGTATGACGAG	AGCCACGAATCTAACTTGTGATG	274 bp
Histone 3.2	CGTCCAGGAACAGTCGCTCTT	TTCACAGCCTACGCCCTCTCT	293 bp
PpMdhar1	GCACGAGAGCAGCCTACTGTG	AGCACACCAATGGGACAAATC	178 bp
PpMdhar2	CCGAGAACAACCGTCTGTGA	GACGAGAAACGCACCACCAA	182 bp
PpMdhar3	ACGATGGCAAAGTAGTGGGTG	CTAAACAAGTCGTGTGGATTAGC	179 bp
PpMdhar3a	GGGCACGCTGTGAATCGTT	TGGAAACCAGGGAGCCTTGC	251 bp
PpMdhar3b	GGCACGCTGTGAATCCAGG	TGGAAACCAGGGAGCCTTGC	253 bp
PpMdhar3c	GGCTCGGATCCGTCAGG	TGGAAACCAGGGAGCCTTGC	289 bp
PpMdhar3d	TGTTTGATGAAGGTTTTTGAATAT	TGGAAACCAGGGAGCCTTGC	247 bp
PpMdhar3e	ATTTGAGGAAGTGTGGGAAGC	TGGAAACCAGGGAGCCTTGC	296 bp

Table 2. Distribution and characteristics of the 5' UTR splice forms.

	Splice variant	Un-treated	Cytokinin-treated	Auxin-treated	Nr of preAUGs	-ΔG (kcal/mol)
PpMdhar1	*-1a*	0	1	4	2	-26.1
	-1b	0	4	1	1	-21.0
	-1c	0	1	0	1	-34.2
PpMdhar2	*-2a*	0	2	5	0	-22.8
	-2b	2	0	1	0	-23.5
	-2c	0	0	2	0	-10.3
PpMdhar3	*-3a*	0	3	4	1	-85.8
	-3b	1	0	4	1	-85.4
	-3c	1	0	0	0	-35.3
	-3d	1	0	1	4	-46.6
	-3e	1	0	2	4	-70.1

All 5' EST sequences obtained in the study by Nishiyama et al., 2003 were grouped according to whether they originated from cytokinin, auxin or untreated tissue. The free energy of the secondary folding of the splice forms was calculated using *m*fold (3.1; Zucker, 2003) and the ΔG of the most stable fold presented.

Figure legends

Figure1

Alternative splicing of the 5' UTR of *PpMdhar1*, *PpMdhar2* and *PpMdhar3*. (A) The cDNA sequences obtained from ESTs where aligned with the genomic sequence of *PpMdhar1*, *PpMdhar2* and *PpMdhar3*. Introns are indicated with a gray line and exons as solid gray boxes. The length is shown in bp. Although no ESTs were found, PCR analysis of cDNA revealed that a variant of *PpMdhar3c* also exists where a 339 bp is spliced out instead of a 342 bp. (B) Genomic southern blot analysis of *PpMdhar1*(1), *PpMdhar2* (2) and *PpMdhar3* (3). Genomic DNA was digested with DraIII and SpeI and hybridised with a probe specific to the 3' terminal exon of *PpMdhar1*, *PpMdhar2* or *PpMdhar3*. The molecular sizes of the standards are indicated on the left.

Figure 2

Evolution of plant MDHARs. (A) The phylogenetic tree was computed based on a protein distance matrice and generated using WEIGHBOR. Local bootstrap probabilities (1000 replicates) are shown in percent above the branch line (only values ≥50% are indicated). The vertical bars refer to subfamilies according to (Sano et al., 2005). The sequences originate from *Arabidopsis thaliana* (At), *Chlamydomonas reinhardtii* (Cr), *Gossypium sp*. (Gs), *Hordeum vulgare* (Hv), *Medico truncatula* (Mt), *Oryza sativa* (Os), *Physcomitrella patens* (Pp), *Pinus pinaster* (Pin), *Populus trichocarpa* (Pt), *Tortula ruralis* (Tr), *Triticum aestivum* (Ta) and *Zea mays* (Zm). (B) Alignment of partial CerMDHAR sequence (AAD28178.1) from *Ceratopteris richardii* (fern) with cytosolic (AtMDHAR1), membran-bound peroxisomal (AtMDHAR4) and chloroplast/mitochondrial (AtMDHAR5) from *Arabidopsis*.

Figure 3

Gene structure of *Mdhar* representatives from algae, non-vascular and vascular plants. *PpMdhar1*, *PpMdhar2* and *PpMdhar3* were cloned from genomic DNA. The sequences were aligned with their respective cDNA sequences to determine the intron-exon structure. The gene structure of MDHARs from *Arabidopsis thaliana*, *Oryza sativa*, *Populus trichocarpa* and *Chlamydomonas reinhardtii* was obtained by BLAST searches at NCBI (http://www.ncbi.nlm.nih.gov) or JGI (http://genome.jgi-psf.org). Exons are shown as grey boxes and the introns as a grey line. The exon lengths in nucleotides are indicated and introns are shown to scale except the hatched intron in *PtMdhar3*.

Figure 4.

Developmental differences in expression of *PpMdhar1*, *PpMdhar2* and *PpMdhar3*. RNA was extracted from one week old protonema (gray) and five week old gametophytes (white) and used for cDNA synthesis and qRT-PCR. The mRNA copy number was normalised using four housekeeping genes encoding histone (*His3*), elongation factor (*eF1α*), actin (*Act2*) or tubulin (*Tub1*). The data represent an average of 6-8 measurements.

Figure 5

Transcription pattern of *PpMdhar1* (A), *PpMdhar2* (B) and *PpMdhar3* (C) under abiotic stress or after ABA treatment. One week old protonema was exposed to 50 µM ABA (triangle, stippled line), 30 mM 1,500 PEG (square, stippled line), 60 mM NaCl (circle, stippled line), 100 mM NaCl (cross, stippled line), UV-B (triangle, solid line), 100 µM MeV (square, solid line), cold (circle, solid line) or not treated (cross, solid line). Samples were snap frozen in liquid nitrogen, RNA purified and cDNA synthesised. The expression level of *PpMdhar1*, *PpMdhar2* and *PpMdhar3* were determined by qRT-PCR and normalised to four housekeeping genes encoding histone (*His3*), elongation factor (*eF1α*), actin (*Act2*) or tubulin (*Tub1*). The data points represent an average of three measurements.

Figure 6

The expression level of the 5' UTR alternative splice forms of *PpMdhar3*. The qRT-PCR was performed on RNA from one week old protonema exposed to 50 µM ABA (triangle, stippled line), 100 mM NaCl (cross, stippled line), 100 µM MeV (square, solid line), cold (circle, solid line) or not treated (cross, solid line) using a reverse primer specific to the coding region of *PpMdhar3* and a forward primer specific to *PpMdhar3a* (A), *PpMdhar3b* (B), *PpMdhar3c* (C), *PpMdhar3d* (D) and *PpMdhar3e* (E). Prior to use for qRT-PCR each primer set was tested against cDNA clones containing the 5 splice forms to ensure specificity. The data points represent an average of three measurements.

Figure 7

Putative ABA regulatory elements (ABRE; *) and ABA coupling elements (CE;#) in the promoter of *PpMdhar1*, *PpMdhar2* and *PpMdhar3*. (A) The promoter of *PpMdhar1* and *PpMdhar2* showed high similarity and were aligned. (B) The *PpMdhar3* promoter did not show a significant similarity to *PpMdhar1* or *PpMdhar2*. Putative *cis*-elements are indicated with a solid box and mutated *cis*-elements in *PpMdhar2* no longer encoding the consensus sequence with a stippled box.

Figure 1

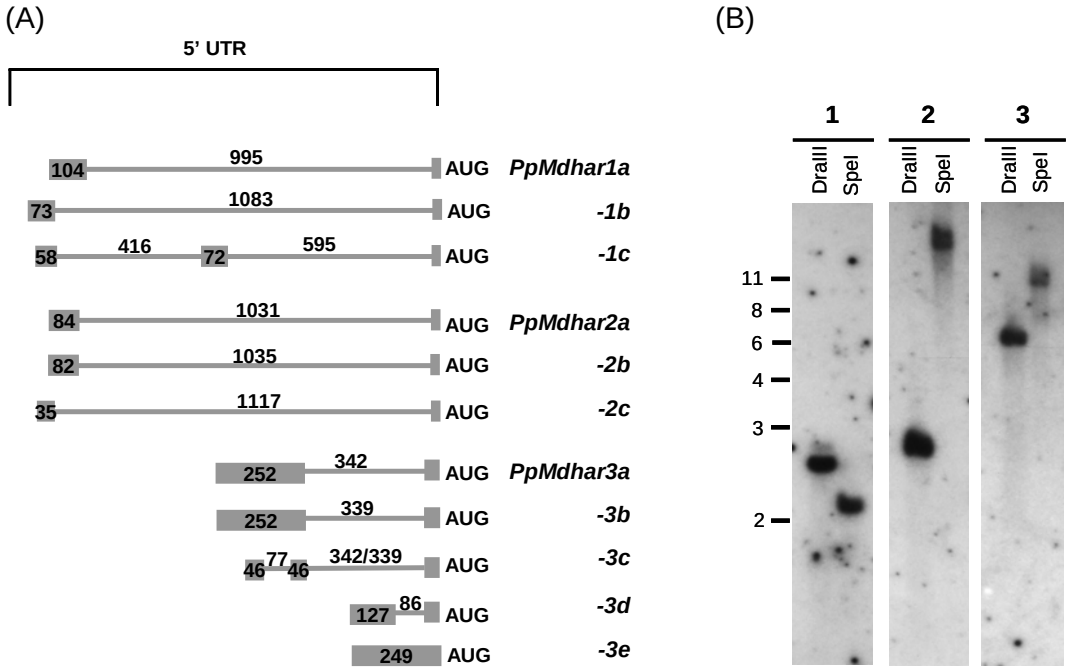
(A)
5' UTR
104
995
AUG
PpMdhar1a
73
1083
AUG
-1b
58
416
72
595
AUG
-1c
84
1031
AUG
PpMdhar2a
82
1035
AUG
-2b
35
1117
AUG
-2c
252
342
AUG
PpMdhar3a
252
339
AUG
-3b
46
77
46
342/339
AUG
-3c
127
86
AUG
-3d
249
AUG
-3e
(B)
1
2
3
DraIII
SpeI
DraIII
SpeI
DraIII
SpeI
11
8
6
4
3
2

Figure 2

(A)

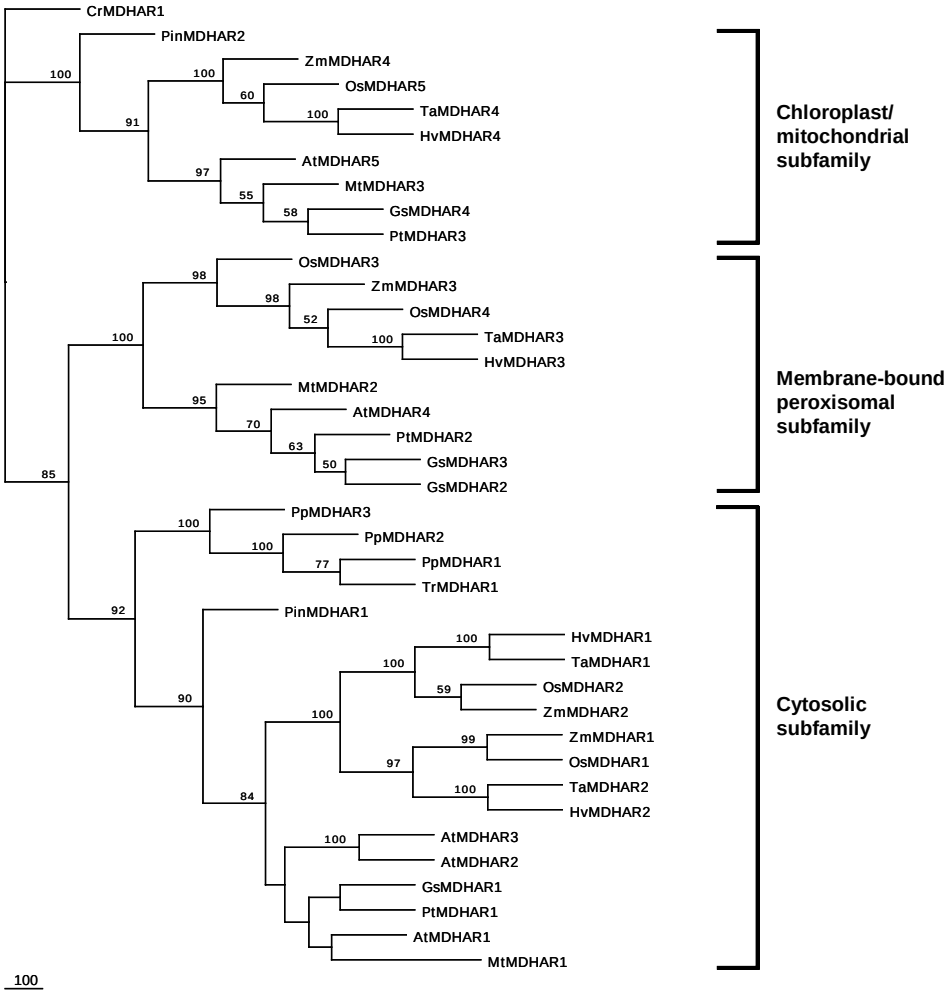

(B)

```
AtMDHAR1 (271) QVEEDK-GGIKTDAFFKTSVPDVYAVGDVATFPLKMYGDVRRVEHVDHSRKSAEQA
AtMDHAR4 (270) QLTIEK-GGIKVNSRMQSSDSSVYAIGDVATFPVKLFGEMRRLEHVDSARKSARHA
AtMDHAR5 (317) LAMNKSIGGIQVDGLFRTSTPGIFAIGDVAAFPLKIYDRMTRVEHVDHARRSAQHC
CerMDHAR2   (1) -GLKMSEGGIEVDGQFRTSSPNVWAIGDVAAFPLKIYNRITRVEHVDHARKSAQHC

                VKAIKAAEGGAAVEEYDYLPFFYSRSFDLS-------WQFYGDNVGDSVLFGDSN-
                VSAIMDPIK---TGDFDYLPFFYSRVFAFS-------WQFYGDPTGDVVHFGEYE-
                VKSLLTAHT----DTYDYLPYFYSRVFEYEGSPRKVWWQFFGDNVGETVEVGNFD-
                VESLLKVQQ----DPYDYLPYFYSRVFEHPGSERKVWWQFYGDNVGDVVEVGDF--
```

Figure 3

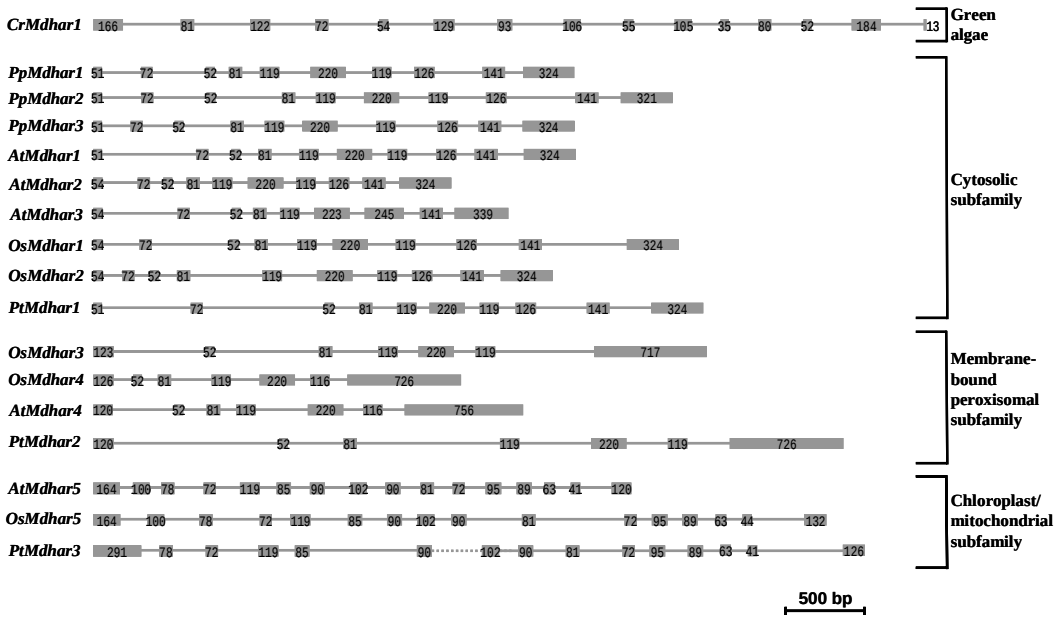
CrMdhar1 166 81 122 72 54 129 93 106 55 105 35 80 52 184 13
PpMdhar1 51 72 52 81 119 220 119 126 141 324
PpMdhar2 51 72 52 81 119 220 119 126 141 321
PpMdhar3 51 72 52 81 119 220 119 126 141 324
AtMdhar1 51 72 52 81 119 220 119 126 141 324
AtMdhar2 54 72 52 81 119 220 119 126 141 324
AtMdhar3 54 72 52 81 119 223 245 141 339
OsMdhar1 54 72 52 81 119 220 119 126 141 324
OsMdhar2 54 72 52 81 119 220 119 126 141 324
PtMdhar1 51 72 52 81 119 220 119 126 141 324
OsMdhar3 123 52 81 119 220 119 717
OsMdhar4 126 52 81 119 220 116 726
AtMdhar4 120 52 81 119 220 116 756
PtMdhar2 120 52 81 119 220 119 726
AtMdhar5 164 100 78 72 119 85 90 102 90 81 72 95 89 63 41 120
OsMdhar5 164 100 78 72 119 85 90 102 90 81 72 95 89 63 44 132
PtMdhar3 291 78 72 119 85 90 102 90 81 72 95 89 63 41 126
500 bp
Green algae
Cytosolic subfamily
Membrane-bound peroxisomal subfamily
Chloroplast/ mitochondrial subfamily

Figure 4

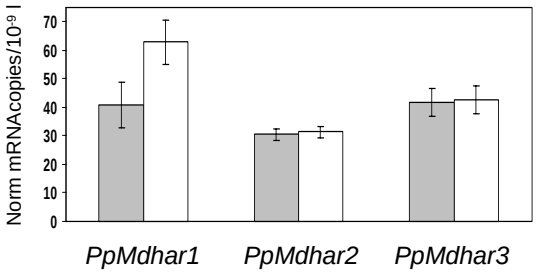
Norm mRNAcopies/10-9 l
70
60
50
40
30
20
10
0
PpMdhar1
PpMdhar2
PpMdhar3

Figure 5

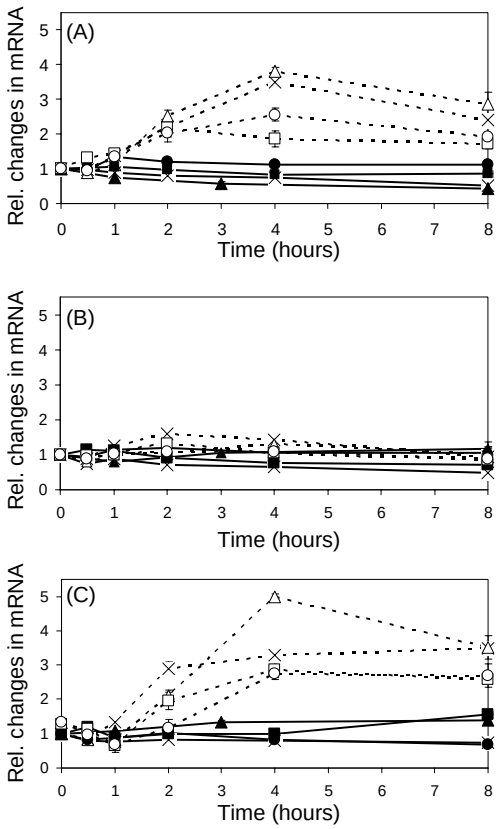
(A)
Rel. changes in mRNA
Time (hours)
(B)
Rel. changes in mRNA
Time (hours)
(C)
Rel. changes in mRNA
Time (hours)

Figure 6

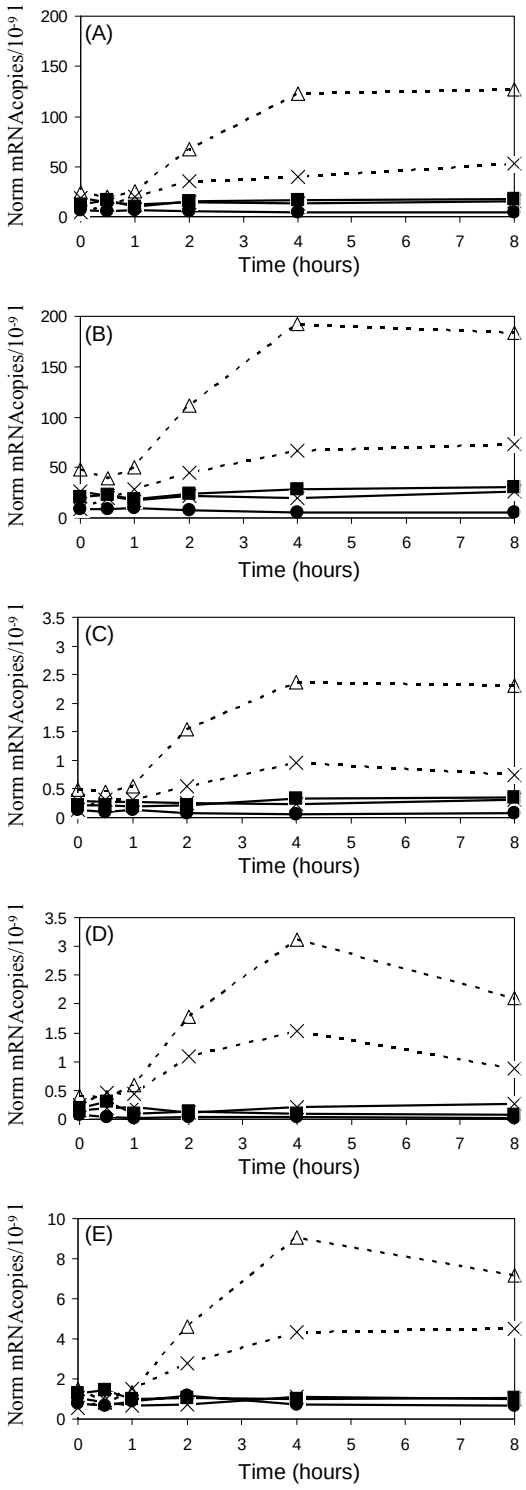

Figure 7

(A)

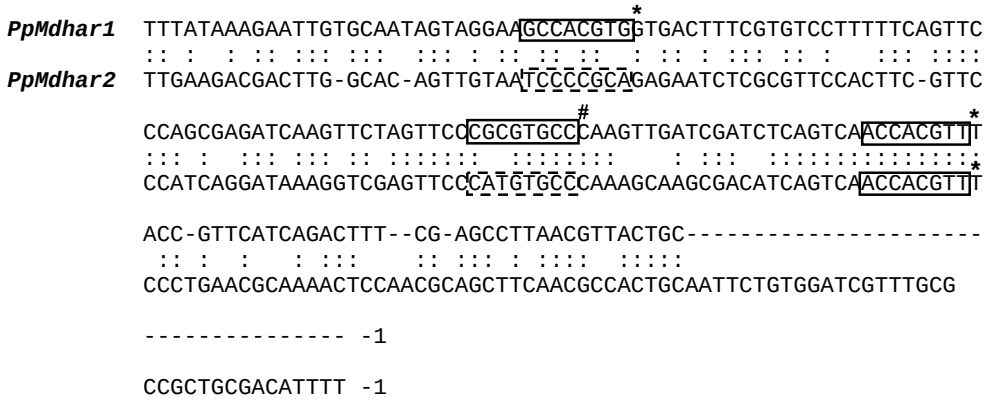
PpMdhar1
PpMdhar2
PpMdhar1
PpMdhar2
PpMdhar1
PpMdhar2
-1
-1

(B)

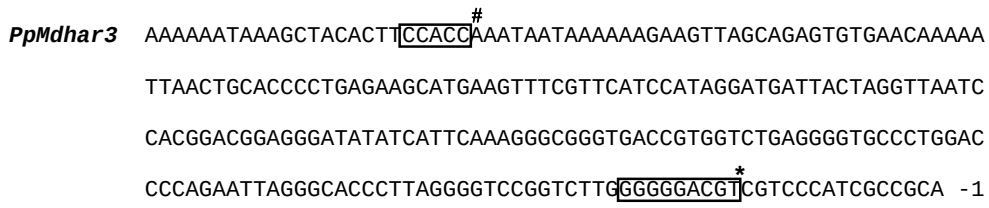
PpMdhar3
-1

Table 1

PCR primers and PCR product sizes in basepairs for the genes analysed			
Gene/Splice variant	**Forward primer**	**Reverse primer**	**PCR size**
β-tubulin-1	GAGTTCACGGAAGCGGAGAG	ATATCTTTCAGGCTCCACCG	224 bp
Elongation factor-1α	GCCAAGAAGAAGTGAATAGTGCG	ACGTCTGCCTCGCTCTAGC	166 bp
Actin-2	GCGAAGAGCGAGTATGACGAG	AGCCACGAATCTAACTTGTGATG	274 bp
Histone 3.2	CGTCCAGGAACAGTCGCTCTT	TTCACAGCCTACGCCCTCTCT	293 bp
PpMdhar1	GCACGAGAGCAGCCTACTGTG	AGCACACCAATGGGACAAATC	178 bp
PpMdhar2	CCGAGAACAACCGTCTGTGA	GACGAGAAACGCACCACCAA	182 bp
PpMdhar3	ACGATGGCAAAGTAGTGGGTG	CTAAACAAGTCGTGTGGATTAGC	179 bp
PpMdhar3a	GGGCACGCTGTGAATCGTT	TGGAAACCAGGGAGCCTTGC	251 bp
PpMdhar3b	GGCACGCTGTGAATCCAGG	TGGAAACCAGGGAGCCTTGC	253 bp
PpMdhar3c	GGCTCGGATCCGTCAGG	TGGAAACCAGGGAGCCTTGC	289 bp
PpMdhar3d	TGTTTGATGAAGGTTTTTGAATAT	TGGAAACCAGGGAGCCTTGC	247 bp
PpMdhar3e	ATTTGAGGAAGTGTGGGAAGC	TGGAAACCAGGGAGCCTTGC	296 bp

Table 2

	Splice variant	**Un-treated**	**Cytokinin-treated**	**Auxin-treated**	**Nr of preAUGs**	**ΔG (kcal/mol)**
PpMdhar1	*-1a*	0	1	4	2	-26.1
	-1b	0	4	1	1	-21.0
	-1c	0	1	0	1	-34.2
PpMdhar2	*-2a*	0	2	5	0	-22.8
	-2b	2	0	1	0	-23.5
	-2c	0	0	2	0	-10.3
PpMdhar3	*-3a*	0	3	4	1	-85.8
	-3b	1	0	4	1	-85.4
	-3c	1	0	0	0	-35.3
	-3d	1	0	1	4	-46.6
	-3e	1	0	2	4	-70.1